euspen's 17th International Conference & Exhibition, Hannover, Germany, May 2017
www.euspen.eu

A displacement interferometer for the calibration of the silicon lattice parameter

Christoph Weichert[1], Paul Köchert[1], Susanne Quabis[1], Jens Flügge[1]

[1] *Physikalisch-Technische Bundesanstalt (PTB), Bundesallee 100, 38116 Braunschweig, Germany*

christoph.weichert@ptb.de

Abstract
We report on an optical heterodyne interferometer for the calibration of the silicon lattice parameter. Besides its special design, first experiments are explained to reach the targeted uncertainty of 30 pm over a measurement length of 10 mm.

Keywords: Interferometry, Periodic nonlinearities, Thermal stability

1. Introduction

In the framework of the Avogadro project the Avogadro constant has been determined with a relative standard uncertainty of $2 \cdot 10^{-8}$ as one prerequisite for a redefinition of the kilogram [1]. For this the number of atoms within a silicon crystal sphere are counted. A necessary parameter for this purpose is the lattice parameter of silicon. It can be determined by measuring the movement of a silicon lamella with an x-ray and an optical interferometer simultaneously. The most accurate measurements were performed by the INRIM with a relative uncertainty of 1.75 nm/m [2]. PTB has set up a second experiment to back up the results of INRIM with slightly different x-ray and optical interferometers.

2. Design and alignment of the optical interferometer

To realise an optical interferometer at this level of uncertainty, all known influences on interferometric measurements have to be taken into account. One prerequisite is a phase evaluation to meet the required resolution [3]. In our case of a heterodyne interferometer the beat-frequency was chosen to be 4 MHz. It is in a range with minimal influence of the laser intensity noise, which can limit the resolving capability of an heterodyne interferometer system [4]. Additionally, there is a minimal influence of the distortions introduced by the optical fibres at this beat-frequency. The interferometer has to be fibre-fed to separate thermal influences from the x-ray interferometer. During the comparison measurement the thermal expansion of silicon of the intrinsic dead path of the x-ray interferometer, the distance between the mirror and the silicon lamella, limits the achievable uncertainty. Its influence outranks the thermal stability of the optical interferometer by more than a factor of ten.

The light of a frequency-doubled, iodine stabilised Nd:YAG laser [5] is frequency-shifted using two acousto-optic modulators and coupled into two polarisation-maintaining fibres. Delivering each beam of different frequency with its own fibre results in spatially separated input beams at the interferometer setup, which avoids periodic nonlinearities caused by frequency mixing [6].

Both interferometers are placed into a vacuum environment to minimize the influence of the refractive index on the wavelength of light. At a wavelength of $\lambda = 532\ \mathrm{nm}$ and a temperature of $T = 293.15\ \mathrm{K}$ the refractive index of dry air is linearly depending on the pressure with a factor of $2.7 \cdot 10^{-9}\ 1/\mathrm{Pa}$. This factor depends on the composition of the residual gas, which is unknown. Therefore, the pressure was reduced below 0.1 Pa. Besides the refractive index the effective wavelength of the optical interferometer is modified by the wavefront shape and the alignment of the beams [7]. In case of a collimated Gaussian beam the wavefront correction is inversely proportional to the squared beam diameter. The maximal beam diameter is limited by the design of the x-ray interferometer. The realised one is approximately $2\omega = 3{,}3\ \mathrm{mm}$ using collimators with an effective focal length of $f = 28\ \mathrm{mm}$. The adjustment of the collimators was realised in air with the help of a calibrated Shack-Hartmann sensor (SHS) taking the influence of the evacuation into account. This approach provides minimal wavefront deviations and also information about the relative alignment of the beams. The beam alignment and deviations of the idealised parabolic wavefront shape has to be considered besides the basic approximation of $\frac{\Delta\lambda}{\lambda} = \left(\frac{\lambda}{2\,\pi\,\omega}\right)^2 = 2.6 \cdot 10^{-9}$ for the length depending deviation. This can be realised using the measured

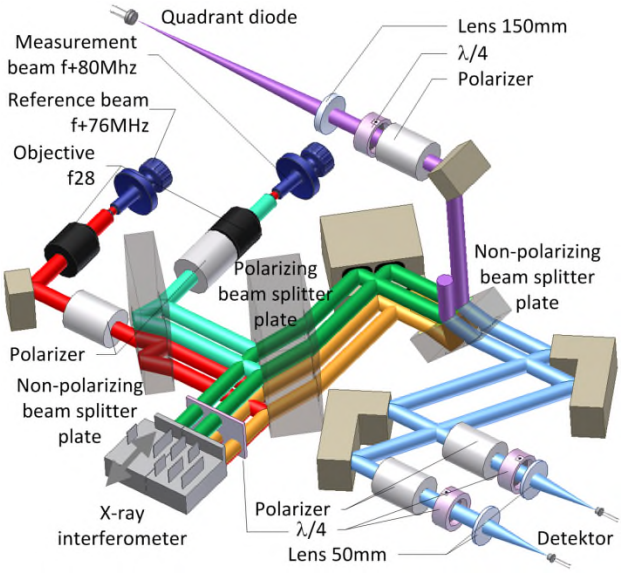

Figure 1. Beam path at the optical interferometer; the spatially separated input beams are marked in turquoise and red.

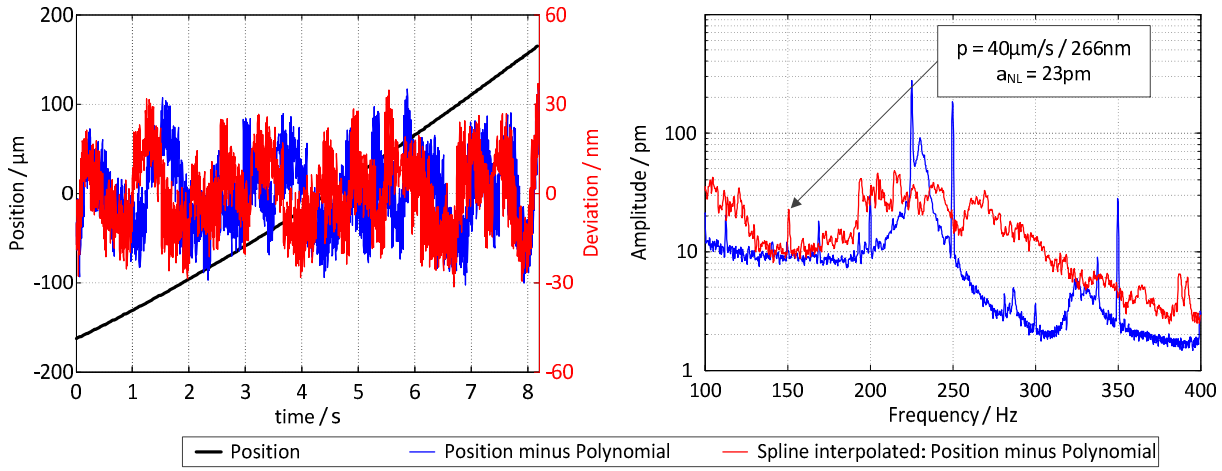

Figure 2. Periodic nonlinearities of the optical interferometer qualified with a non-constant moving speed based on the frequency-domain method.

wavefronts for simulations [8], which also include the exact beam profile defined by the fundamental mode of the single-mode fibres.

The beam paths of the optical interferometer are illustrated in figure 1. They are leaned on previous designs [9] but adapted to evacuated environment conditions. The two collimated input beams each pass a Glan polarizer, which are used to reject the second polarization state of the beams caused by mechanically introduced stress along the optical fibres. A misalignment of these polarizers would result in variations of the measured phase caused by imperfections of the beam splitters and different phase variations of the two guided modes of the optical fibres [10]. The mechanical stress along the fibres additionally leads to different phase variations of the two incoming beams. Therefore, the reference phase has to be picked up behind the fibres. This is realised by splitting the incoming beams with a non-polarizing beam splitter (NPBS) plate, which results in an additional reference interferometer whose beams are reflected only by the reference mirror.

The beams are superposed at another NPBS plate. Half of the light is used to evaluate the mirror movement. Therefore, the superposed beams are focused on photodiodes after they had passed an optical isolator consisting of a polarizer and a quarter-wave plate. Each current signal of the two diodes is amplified and converted using transimpedance amplifiers and analysed with a phase meter [3]. The other half of the reference interferometer light is focused on a quadrant diode. It is used to measure angle variations in the µrad range between the x-ray and the optical interferometer. By means of several determinations of the lattice parameter at different angles between the two interferometers the influence of the cosine error can be minimized [2].

3. Evaluation of the optical interferometer

For the evaluation of the optical interferometer several measurements were performed excluding the x-ray interferometer. In a first step the x-ray interferometer was replaced by one mirror reflecting all the four beams. The phase difference of the two photodiode signals exhibited a standard deviation of 0.28 mrad over 300 seconds at an acquisition rate of 50 kHz, which corresponds to a resolving capability of 12 pm for the single-path interferometer. A long-term analysis of the phase variation while the temperature was changing turned out a thermal dependency of 1.2 nm/K for the optical interferometer. Since the beam paths of the interferometer are balanced and the optics are mounted with minimal introduced stress with holders made of the low expansion steel Invar the most probable reason for the thermal dependency are phase shifts introduced by the transimpedance amplifiers.

In a second step a mirror was mounted on a piezo linear stage to evaluate the periodic nonlinearities. Since the stage was moved by applying a saw tooth voltage to its controller without any feedback loop it offered only a non-constant moving speed, as illustrated in figure 2. To analyse the periodic nonlinearities with the help of an amplitude spectrum according to the frequency-domain method [11] actually a constant moving speed is required, otherwise the estimated amplitude is too small. Therefore a spline-interpolation simulating a constant movement was used to determine the amplitude of the periodic nonlinearities [12]. First a polynomial function was subtracted from the position data and afterwards the resulting residuals were interpolated with a cubic spline at an interpolant constructed based on the average moving speed. The amplitude spectra was now calculated for a vector equidistant in space (red curve) and not in time anymore (blue curve). Therefore the red curve in figure 2 makes the periodic nonlinearities with an amplitude below 25 pm clearly visible by suppressing variations periodically in time. The periodic nonlinearities were mostly caused by multi-reflections. Since the mirror has to be placed orthogonal to the beams in the µrad range, light recycling is giving a limit [13].

Acknowledgement

The authors like to thank their colleagues for supporting the work especially emphasising the contributions of Birk Andreas and Michael Müller.

References

[1] Bettin H et al., 2015, Metrologia **52**(2)
[2] Massa E, Sasso C P, Mana G and Palmisano C, 2015,Journal of Physical and Chemical Reference Data **44**, 031208
[3] Köchert P, et al., 2012, Meas. Sci. Technol., **23**(7)
[4] Weichert C, Köchert P, Köning R and Flügge J, 2014, Proc. of 58th Ilmenau scientific colloquium
[5] Schnatz H and Mensing F, 2001, Proc. SPIE 4269, Laser Frequency Stabilization, Standards, Measurement, and Applications, 239
[6] Tanaka M, Yamagami T and Nakayama K, 1989, IEEE Transactions on instrumentation and measurement, **38**(2)
[7] Cavagnero G, Mana G and Massa E, 2006, J. Opt. Soc. Am. A, **23**(8)
[8] Andreas B, Mana G and Palmisano C, 2015, J. Opt. Soc. Am. A **32**(8)
[9] Weichert C, et al., 2012, Meas. Sci. Technol., **23**(9)
[10] Massa E, et al., 2013, Optics Express, **21**(22)
[11] Badami V G and Patterson S R, 2000, Precis. Eng., **24**(1)
[12] Yang H, Weichert C, Köchert P and Flügge J, 2016, Opt. Lett. **41**(23)
[13] Cavagnero G, Mana G and Massa E, 2005, Rev. Sci. Instrum., **76**(5)